Journal of Magnetics 12(1), 21-26 (2007)

Fully Integrated Electromagnetic Noise Suppressors Incorporated with a Magnetic Thin Film on an Oxidized Si Substrate

Jaecheon Sohn[1], S. H. Han[1], Masahiro Yamaguchi[2], and S. H. Lim[3]*

[1]*Nano Device Research Center, Korea Institute of Science and Technology, P. O. Box 131, Cheongryang, Seoul 130-650, Korea*
[2]*Department of Electrical and Communication Engineering, Tohoku University, Sendai 980-8579, Japan*
[3]*Department of Materials Science and Engineering, Korea University, Seoul 136-713, Korea*

(Received 6 March 2007)

Si-based electromagnetic noise suppressors on coplanar waveguide transmission lines incorporated with a SiO_2 dielectric layer and a nanogranular Co-Fe-Al-O magnetic thin film are reported. Unlike glass-based devices, large signal attenuation is observed even in the bare structure without coating the magnetic thin film. Much larger signal attenuation is achieved in fully integrated devices. The transmission scattering parameter (S_{21}) is as small as –90 dB at 20 GHz at the following device dimensions; the thicknesses of the SiO_2 and Co-Fe-Al-O thin films are 0.1 μm and 1 μm, respectively, the length of the transmission line is 15 mm, and the width of the magnetic thin film is 2000 μm. In all cases, the reflection scattering parameter (S_{11}) is below -10 dB over the whole frequency band. Additional distributed capacitance formed by the Cu transmission line/SiO_2/Si substrate is responsible for these characteristics. It is considered that the present noise suppressors based on the Si substrate are a first important step to the realization of MMIC noise suppressors.

Keywords : electromagnetic noise suppressor, integrated device, Si substrate, coplanar waveguide transmission line, magnetic thin film

1. Introduction

The development of high-frequency devices is important in a technical point of view because of the increasing volume of information and the variety of communication media, such as mobile telephones and satellite broadcasting systems. The goal of mobile/wireless communications in the coming years is to allow users to access the global network at any time, without regard to mobility or location. Cellular and cordless telephone communications have begun this process and continued developments in satellite communications, fiber-optic and digital microwave radio communications are aimed at this goal [1]. On the other hand, the electromagnetic radiation in high speed LSIs such as CPU and peripheral microcontrollers becomes a real hot issue, as concern of electromagnetic compatibility (EMC) is expanding to a wide variety of downsized circuit devices. The so-called micro-EMC, the EMC solution in the near field, is attracting a wide interest, the main subjects of which include microscopic techniques of electromagnetic measurements and methods to cope with the radiation noise. Harmonic noise suppressors play a key role in micro EMC and passive harmonic suppressors among them come in a wide variety. Conventionally, lumped element chips such as inductors, capacitors, and resistors have been the main components of suppressor to filter the harmonic noise [2]. However, due to their own self-resonance, the lumped elements cannot be used in monolithic microwave integrated circuits (MMICs) with their operating frequency in the GHz range. Therefore, distributed elements should be adopted instead. Many efforts have been made to downsize noise suppressors and the ultimate can be MMIC suppressors fabricated on a Si or GaAs substrate, with an obvious advantage of the integration of noise suppressors with other semiconductor IC devices. An example of downsizing process with the use of MMIC suppressors is illustrated in Fig. 1, where it is seen that IC chips are combined to form MMIC chips.

Recently, good signal attenuation characteristics combined with the high resonance frequencies of approximately 10 GHz were observed in integrated-type noise suppressors utilizing a nanogranular Co-Fe-Al-O magnetic thin film, making them suitable for high frequency noise suppressors

*Corresponding author: Tel: +82-2-3290-3285,
Fax: +82-2-928-3584, e-mail: sangholim@korea.ac.kr

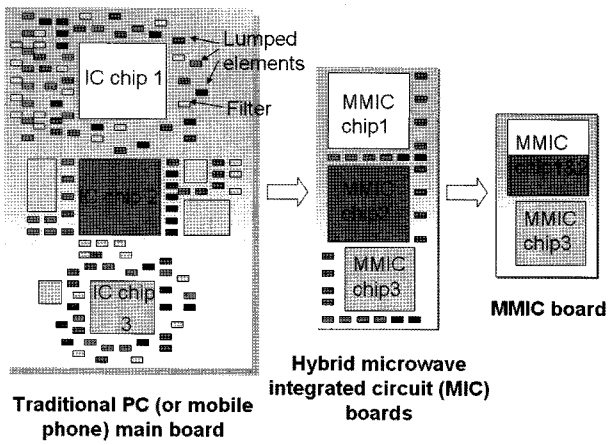

Fig. 1. An example of a downsizing process with the use of MMIC suppressors.

[3, 4]. The main mechanism for the generation of loss was found to be the *L-C* resonance. In previous similar devices, however, the main loss mechanism was considered to be ferromagnetic resonance (FMR) with a secondary role played by eddy currents [5-9]. All these previous noise suppressors do not perform in MMIC devices, because they are based on a glass substrate. In this work, a similar device of a coplanar waveguide transmission line integrated with a SiO_2 dielectric layer and a nano-granular Co-Fe-Al-O magnetic thin film is reported, but the main difference is the use of an oxidized Si substrate. Some typical results are to be published in the literature [10].

2. Experiments

The coplanar transmission line with a characteristic impedance of 50 Ω was designed on a Si substrate (the relative permittivity, $\varepsilon_r = 11.9$) coated with an insulating SiO_2 layer by using the Muller and Hilberg equation [11]:

$$Z_0 = \frac{\eta_0}{4.0\sqrt{\varepsilon_{eff}}} \frac{1}{[K(k_1')/K(k_1)] + (t/b - a)}$$

$$\varepsilon_{eff} = 1 + \frac{\varepsilon_r - 1}{2} \frac{K(k_2')/K(k_2)}{[K(k_1')/K(k_1)] + (t/b - a)}. \quad (1)$$

Eq. (1) gives the characteristic impedance (Z_0) and effective permittivity (ε_{eff}) of the coplanar line. Here, a, b, c, and t are the cross-sectional dimensions of the transmission line, as shown in Fig. 2(a), and k_1, k_1', k_2, and k_2' are the functions of the cross-sectional dimensions. The overall stack consisted of a nanogranular Co-Fe-Al-O magnetic thin film (1 μm)/SiO_2 (0.1 μm)/Cu transmission line (3 μm)/SiO_2 (2.5 μm)/Si-substrate (500 μm). The insulating SiO_2 layer just above the Si substrate is necessary because the substrate is not a complete insulator. In

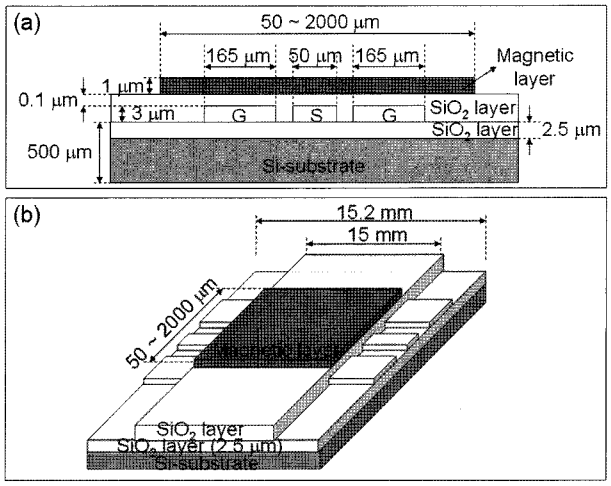

Fig. 2. (a) A cross-sectional view of the CPW transmission line, together with the dielectric and magnetic layers, on a Si substrate coated with a SiO_2 layer. (b) A schematic showing the overall device structure. Note that the dimensions are not in a proper scale.

this work, a standard B-doped p-type Si was used as the substrate. Of course, no insulating layer is required if a glass is used as the substrate [3, 4]. A cross-sectional view of the designed transmission line is shown in Fig. 2(a) together with the dielectric (SiO_2) and magnetic layers. A schematic showing the overall device structure is displayed in Fig. 2(b). Note that the dimensions in Figs. 2(a) and (b) are not in a proper scale. It should be noted that the length of the transmission line is 0.2 mm longer than that of the dielectric and magnetic layers in order to provide room for electrical contact. However, it is specified by the length of the dielectric and magnetic layers throughout this paper just for convenience. A conventional microfabrication process including photolithography and wet etching was used to fabricate the integrated device. The Cu transmission lines were deposited by electroplating in an electrolyte composed of $CuSO_4$, H_2SO_4, and DI water. Before the Cu plating, very thin seed layers of Cu (0.06 μm)/Ti (0.01 μm) were deposited by RF sputtering onto the SiO_2 layer. Also, a very thin Ti layer with a thickness of ~10 nm was deposited between the upper SiO_2 layer and magnetic thin film for an improved adhesion of the magnetic layer. A nanogranular magnetic film with the composition $Co_{41}Fe_{38}Al_{13}O_8$ (in atomic %) was deposited by RF magnetron sputtering under a static magnetic field of 1 kOe to form an induced anisotropy [12, 13]. After photo-resist patterning, the magnetic film was etched by ion milling. A wet etching method was finally used to remove the SiO_2 layer on the contact pad at both ends of the transmission line by using a buffered oxide etch solution (HF:H_2O= 1:6). For measurements, two ground-signal-ground (GSG)

pin type wafer probes were in mechanical contact with both ends of the CPW transmission line. The *S*-parameters (S_{11} and S_{21}) were measured with a HP 8720D network analyzer in the frequency range of 0.1 to 20 GHz.

3. Results and Discussion

The present $Co_{41}Fe_{38}Al_{13}O_8$ nanogranular thin film exhibits excellent soft magnetic properties at high frequencies and important properties are summarized as follows [12, 13]: an electrical resistivity (ρ) of 374 $\mu\Omega$cm, an anisotropy field (H_K) of 50 Oe, a hard axis coercivity of 1.25 Oe, and a saturation magnetization ($4\pi M_S$) of 12.9 kG, and a resonance frequency (f_R) of 2.24 GHz.

Figs. 3(a)~(c) respectively show the frequency dependences of the transmitted (S_{21}) and reflected (S_{11}) scattering parameters and the fraction of power loss (P_{loss}/P_{input}) for the "bare" CPW transmission lines with various lengths of 2, 5, 10 and 15 mm. The bare structure indicates no dielectric (SiO_2) and magnetic (Co-Fe-Al-O) layers above the transmission line. Geometrically, the bare structure based on the present Si substrate is similar to that based on a glass substrate in that there are no dielectric (SiO_2) and magnetic (Co-Fe-Al-O) layers coated above the transmission line. However, in the view point of wave transmission, a large difference is expected mainly due to the existence of a possible distributed capacitor in the Si-based device formed by the Cu transmission line and the layers below it; namely, the Cu transmission line/SiO_2/Si substrate. The semiconducting Si can act as a capacitor electrode, particularly in high frequencies.

It is seen from Fig. 3(a) that, for a given transmission line length (l), the signal attenuation increases monotonically with increasing frequency, except for a small plateau near 2 GHz at l=10 and 15 mm. At a given frequency, the attenuation increases with increasing transmission line length, this tendency being more obvious at higher frequencies. At the lowest measured frequency of 100 MHz, no obvious difference is seen in the signal attenuation depending on the length, but the difference begins to appear at 200 MHz. At l=2 mm, only a moderate frequency dependence of the signal attenuation is observed over the whole frequency range, but, at higher lengths, rather steep signal attenuation begins to occur at certain frequencies: 6 GHz at l=5 mm and 2~3 GHz at l=10 and 15 mm. The magnitudes of signal attenuation at the highest measured frequency of 20 GHz are; −7.5 dB at l=2 mm, −16 dB at l=5 mm, −33.5 dB at l=10 mm, and −50 dB at l=15 mm. The present frequency dependence of the signal attenuation showing the monotonic behavior indicates the absence of resonance in the measured frequency range, possibly due to the absence or a small magnitude of distributed inductance component in the present bare structure.

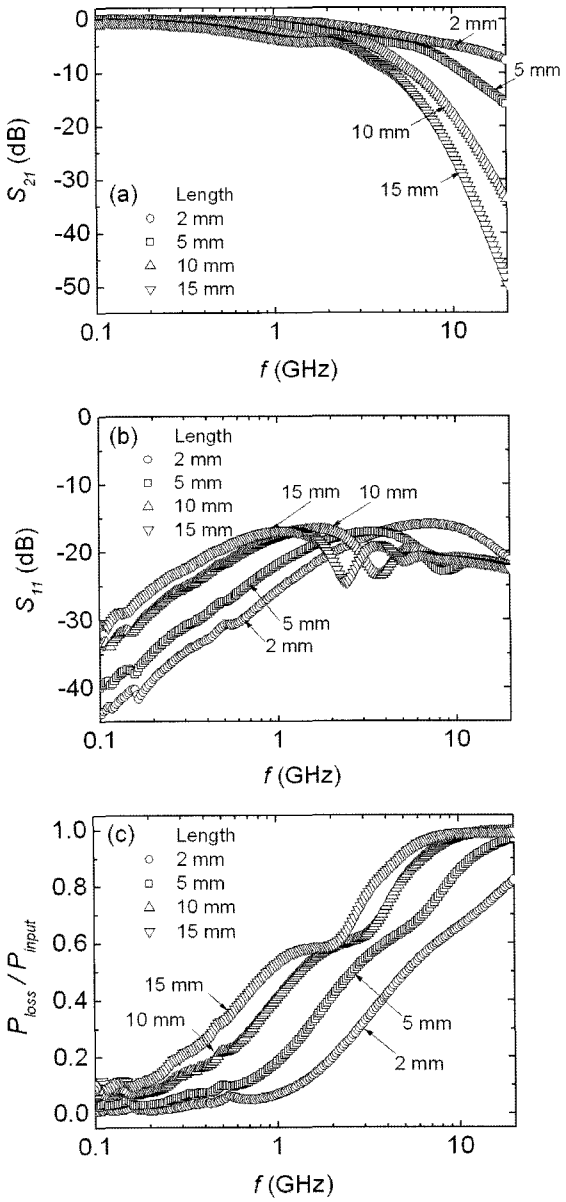

Fig. 3. The frequency dependences of (a) S_{21}, (b) S_{11}, (c) the fraction of power loss (P_{loss}/P_{input}) for the Si-based bare CPW transmission lines with various lengths of 2, 5, 10 and 15 mm. The coplanar transmission lines are fabricated on an oxidized substrate, SiO_2 (2.5 μm)/Si (500 μm).

The amount of reflected signal (S_{11}), as can be seen from Fig. 3(b), is relatively small being less than −15 dB in all cases. At low frequencies, the magnitude of reflected signal increases progressively with increasing length. At high frequencies, however, no obvious tendency is seen, mainly due to the appearance of sharp minima (dips) in S_{11}. These dips are known to be caused by dimensional resonance losses which occur when the length of the

transmission line is an integer multiple of the half guided wavelength of the electromagnetic wave [14-17]. In the high frequency range, the value of S_{11} is in the range of −15 to −25 dB in all cases. The power loss (P_{loss}) can be calculated from the scattering parameters by using the equation; $P_{loss}/P_{input}=1-(|S_{21}|^2+|S_1|^2)$, where P_{input} is the input power. The power loss is higher at longer line lengths, as can be seen from Fig. 3(c), and, at a given length, it increases with increasing frequency. In all cases, the increase is slow initially, followed by a steeper increase at intermediate frequencies. The frequency showing the steep increase is 1 GHz at l=2 mm and it is decreased to 200 MHz at larger lengths, l=10 and 15 mm. Similarly to S_{21}, there is a plateau near 2 GHz in the frequency dependence of the power loss at l=10 and 15 mm, although the reason for this is not understood at the moment. The power loss saturates to a value of approximately 100% at frequencies well below 10 GHz in the cases of l=10 and 15 mm, but, at shorter lengths, no saturation occurs.

It is of interest to compare the present results for the bare transmission lines based on the Si substrate with those for the bare structure based on a glass substrate as shown in Figs. 4(a) and (b), respectively for S_{21} and S_{11}, and the power loss [3, 4]. The results in Figs. 4(a)~(c) are plotted in a way similar to Figs. 3(a)~(c). The two sets of results in Figs. 3 and 4 are at least qualitatively similar to each other. For example, both the signal attenuation (over the whole frequency range) and reflection (at low frequencies below dimensional resonance) increase with increasing transmission line length, and the power loss increases monotonically with increasing frequency. However, they are strikingly different in quantitative terms. In the case of the bare structures based on a glass substrate, the attenuation of the transmitted signal is very small over the whole frequency range (at low frequencies in particular), the highest being −2.3 dB at the highest frequency of 20 GHz and the largest length of 15 mm. Also, the amount of reflected signal is also very small being less than -30 dB in all cases. The main reason for the large difference may result from the formation of a distributed capacitor even in the bare transmission line based on the Si substrate, as was discussed before. In the case of the bare structure based on a glass substrate, there is no capacitor component since the Cu transmission line is directly on top of a dielectric glass. The scattering parameters and the power loss in this case can mainly be explained by the eddy current losses with a minor contribution from the distributed inductance of the Cu transmission line itself. Another factor may be that Si has a much higher relative dielectric constant (ε_r=11.9) than a Corning glass #7059 (ε_r=5.84) used as the substrate. With its high dielectric

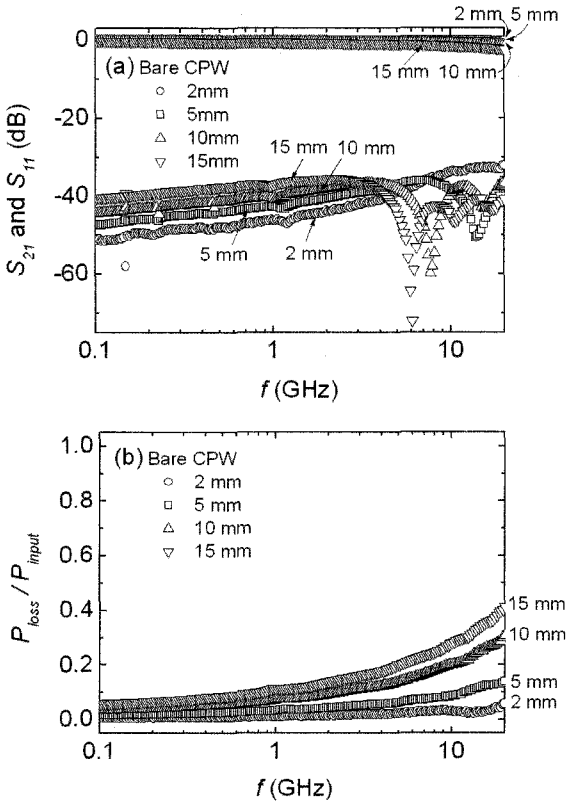

Fig. 4. The frequency dependences of (a) S_{21} and S_{11} and (b) the fraction of power loss (P_{loss}/P_{input}) for the bare CPW transmission lines on a glass substrate with various lengths of 2, 5, 10 and 15 mm [3, 4].

constant, Si can absorb more energy than glass during the transmission of the electromagnetic wave, although this effect is expected to be small.

The dielectric and magnetic thin films were coated on the bare structure to form complete integrated devices and the results for the frequency dependences of the signal attenuation, signal reflection, and power losses, respectively, are shown in Figs. 5(a)~(c). The thicknesses of the SiO_2 and Co-Fe-Al-O thin films are 0.1 μm and 1 μm, respectively. The length of the transmission line was fixed at 15 mm (the largest), but the width of the magnetic thin film was varied from 50 to 2000 mm. With the additional dielectric and magnetic layers on top of the transmission line, another distributed capacitor can be formed by the trilayers, the Cu transmission line/SiO_2 dielectric layer/ Co-Fe-Al-O magnetic thin film, and also a new distributed inductor by the magnetic thin film. These additional components are expected to affect the transmission and reflection characteristics and indeed this expectation is clearly met from the results shown in Figs. 5(a)~(c).

It is seen from Fig. 5(a) that the signal attenuation is increased with the incorporation of the dielectric and magnetic layers. As the width of the magnetic film (w)

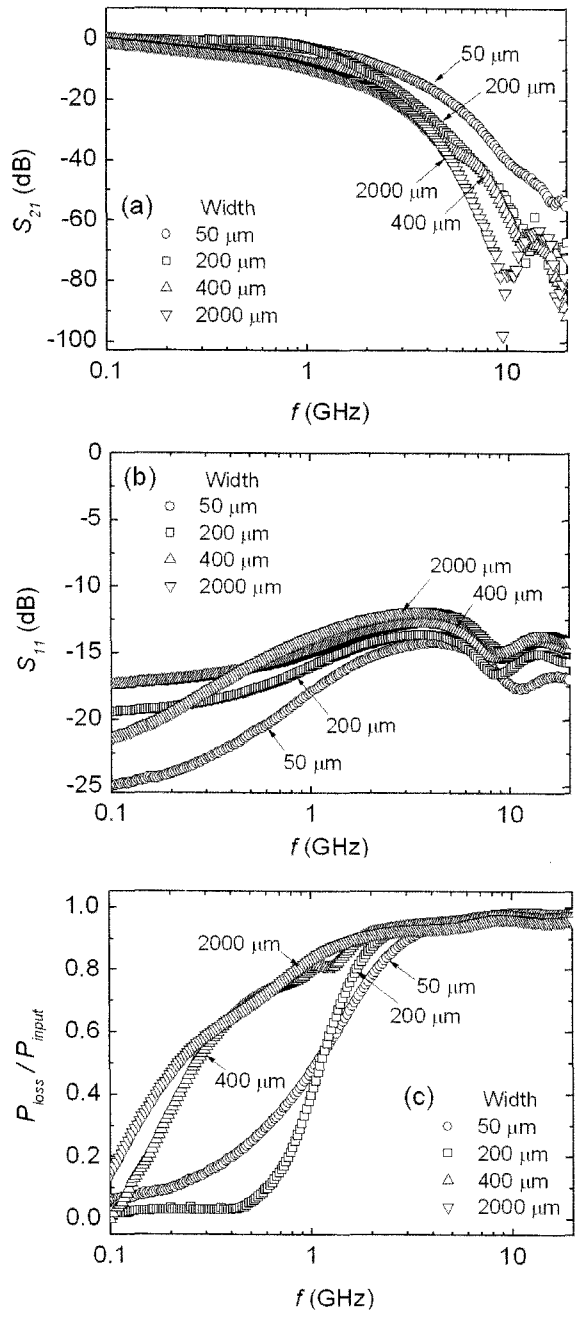

Fig. 5. The frequency dependences of (a) S_{21}, (b) S_{11}, and (c) the fraction of power loss (P_{loss}/P_{input}) for the Si-based noise suppressors integrated with the dielectric (0.1 μm-thick) and magnetic (1 μm-thick) layers above the Cu transmission lines. The layers below the coplanar transmission lines are those from an oxidized substrate, SiO_2 (2.5 μm)/Si (500 μm). The length of the magnetic thin film is fixed at 15 mm, but the width of the magnetic thin film is varied as 50, 200, 400, and 2000 μm.

increases, the signal attenuation also tends to increase continuously, except for the w=200 μm device where the signal attenuation is even smaller than for the w=50 μm sample in the low frequency range below 1 GHz, although this is not clearly seen in the figure due to a large scale of the y axis. Similarly to the bare structure, the signal attenuation also tends to increase with increasing frequency, although this behavior is not very definite at large widths and high frequencies above 10 GHz where minima in S_{21} are observed. The signal attenuation begins to increase at 150~200 MHz for the w=400 and 2000 μm devices, while at 600~900 MHz for the w=50 and 200 μm samples. The value of S_{21} is approximately −80 ~ −90 dB for all samples, except for the w=50 μm one, at the highest measured frequency of 20 GHz. To the best of our knowledge, this level of signal attenuation is probably the highest for the RF noise suppressors with similar lateral dimensions. At w=50 μm, the value of S_{21} is about −55 dB, this level being also large considering the small volume of the dielectric and magnetic layers on top of the coplanar transmission line.

From Fig. 5(b), it is observed that the amount of signal reflection tends to increase with increasing width, a behavior similar to those observed previously [4]. At low frequencies below 500 MHz, however, this tendency is not observed; this is mainly because, at w=2000 μm, the signal reflection decreases relatively steeply with decreasing frequency, while a small frequency dependence is observed at w= 200 and 400 μm. In all cases, the value is S_{11} are below −10 dB in the whole frequency band, implying that the input signal distortion due to the reflected signals may not be serious when used as noise suppressors. The power loss, shown in Fig. 4(c), is generally higher at larger widths of the magnetic thin film, with the notable exception for the results at w=200 μm, where the power loss is even smaller than that at w=50 μm at frequencies below 1 GHz. This behavior is consistent with the signal attenuation result. At w=50 and 200 μm, the power loss increases slowly in the low frequency range, in particular at w=200 μm, where it virtually remains constant up to 600 MHz. The slow increase is followed by a steep increase at intermediate frequencies. The frequency dependence of the power loss at w=400 and 2000 μm is different from that at lower widths; in this case, a logarithmic increase is observed. In all cases, saturation occurs at 2~4 GHz and saturated value is 90~100%.

4. Conclusions

The Si-based CPW transmission lines integrated with a SiO_2 dielectric and a nanogranular Co-Fe-Al-O magnetic thin film are found to exhibit very good characteristics for noise suppressors. The value of S_{21} is as low as −90 dB at the highest measured frequency of 20 GHz and this level

of signal attenuation is probably among the highest for the RF noise suppressors with similar lateral dimensions. The signal reflection is relatively small being below −10 dB. An additional distributed capacitance resulting from the layers consisting of the Cu transmission line and the oxidized Si substrate is mainly responsible for the noise absorption and reflection characteristics. It is considered that the present Si-based devices, with their good signal attenuation and reflection features, are suitable for MMIC noise suppressors.

Acknowledgments

This work was supported by the Korea Research Foundation (Grant No. D00335).

References

[1] C. K. Campbell, *Surface Acoustic Wave Devices for Mobile and Wireless Communications* (Academic Press, New York, 1998), Chap. 19.
[2] J. S. Hong and M. J. Lancaster, *Microstrip Filters for RF/Microwave Applications* (John Wiley & Sons, New York, 2001), Chaps. 5 & 6.
[3] J. C. Sohn, S. H. Han, M. Yamaguchi, and S. H. Lim, Appl. Phys. Lett. **89**, 103501 (2006).
[4] J. C. Sohn, S. H. Han, M. Yamaguchi, and S. H. Lim, J. Appl. Phys. **100**, 124510 (2006).
[5] M. Yamaguchi, Ki-Hyeon Kim, Takashi Kuribara, and Ken-Ichi Arai, IEEE Trans. Magn. **38**, 3183 (2002).
[6] K. H. Kim, M. Yamaguchi, K. I. Arai, H. Nagura, and S. Ohnuma, J. Appl. Phys. **93**, 8002 (2003).
[7] K. H. Kim, M. Yamaguchi, S. Ikeda, and K. I. Arai, IEEE Trans. Magn. **39**, 3031 (2003).
[8] K. H. Kim, M. Yamaguchi, K. I. Arai, N. Matsushita, and M. Abe, Trans. Magn. Soc. Japan **3**, 133 (2003).
[9] J. C. Sohn, S. H. Han, K. H. Kim, M. Yamaguchi, and S. H. Lim, J. Magn. Magn. Mater. **311**, 708 (2007).
[10] J. C. Sohn, S. H. Han, M. Yamaguchi, and S. H. Lim, Appl. Phys. Lett. (Accepted).
[11] B. C. Wadell, *Transmission Line Design Handbook* (Artech House, Boston, 1991), Chap. 3.
[12] J. C. Sohn, D. J. Byun, and S. H. Lim, J. Magn. Magn. Mater. **272-276**, 1500 (2004).
[13] J. C. Sohn, D. J. Byun, and S. H. Lim, Phys. Stat. Sol. (a) **201**, 1786 (2004).
[14] Walter Barry, IEEE Trans. Microwave Theory Tech. **34**, 80 (1986).
[15] W. B. Weir, Proc. IEEE **62**, 33 (1974).
[16] A. M. Nicolson and G. F. Ross, IEEE Trans. Instrum. Meas. **19**, 377 (1970).
[17] R. W. Ziolkowski, IEEE Trans Antennas Propagat. **51**, 1516 (2003).